Serial Femtosecond Crystallography of Membrane Proteins

11

Lan Zhu, Uwe Weierstall, Vadim Cherezov, and Wei Liu

Abstract

Membrane proteins, including G protein-coupled receptors (GPCRs), constitute the most important drug targets. The increasing number of targets requires new structural information, which has proven tremendously challenging due to the difficulties in growing diffraction-quality crystals. Recent developments of serial femtosecond crystallography at X-ray free electron lasers combined with the use of membrane-mimetic gel-like matrix of lipidic cubic phase (LCP-SFX) for crystal growth and delivery hold significant promise to accelerate structural studies of membrane proteins. This chapter describes the development and current status of the LCP-SFX technology and elaborates its future role in structural biology of membrane proteins.

Keywords

Serial femtosecond crystallography • X-ray free electron laser • Lipidic cubic phase • LCP-SFX • LCP injector • Membrane proteins • G protein-coupled receptors

11.1 Introduction

Membrane proteins, accounting for approximately 30 % of all proteins in eukaryotic cells (Wallin and von Heijne 1998), play crucial roles in multiple cellular processes, from transmitting extracellular signals, transporting cellular

L. Zhu • W. Liu (✉)
School of Molecular Sciences, Arizona State University, Tempe, AZ 85287, USA

Center for Applied Structural Discovery at the Biodesign Institute, Arizona State University, Tempe, AZ 85287-1604, USA
e-mail: lan.zhu@asu.edu; w.liu@asu.edu

U. Weierstall
Center for Applied Structural Discovery at the Biodesign Institute, Arizona State University, Tempe, AZ 85287-1604, USA

Department of Physics, Arizona State University, Tempe, AZ 85287, USA
e-mail: weier@asu.edu

V. Cherezov
Bridge Institute, University of Southern California, Los Angeles, CA 90089, USA

Department of Chemistry, University of Southern California, Los Angeles, CA 90089, USA
e-mail: cherezov@usc.edu

© Springer International Publishing Switzerland 2016

I. Moraes (ed.), *The Next Generation in Membrane Protein Structure Determination*, Advances in Experimental Medicine and Biology 922, DOI 10.1007/978-3-319-35072-1_11

components across the membrane, and catalysing chemical reactions, to mediating cellular interactions. Currently, approximately 60 % of approved drugs target membrane proteins, not only due to their vital roles, but also because of the easiness in accessing them at the cell surface (Yildirim et al. 2007). Structure characterization of membrane proteins is fundamental for the comprehensive understanding of their mechanisms of action and biological functions. However, their residence within a lipid bilayer renders great difficulties for the isolation, purification, stabilisation and crystallisation of membrane proteins, and thus makes their structure determination challenging.

The first high-resolution three-dimensional structure of a membrane protein was solved by X-ray crystallographic analysis in 1985 (Deisenhofer et al. 1985). After decades of efforts to develop effective approaches for structure determination, X-ray crystallography stands out as the most efficient tool for high-resolution three-dimensional structure determination of membrane proteins, attributing to over 600 unique membrane protein structures deposited in the Protein Data Bank (http://www.pdb.org). However, compared with soluble proteins, the progress for structure determination of membrane proteins lags far behind. Among the notoriously difficult membrane protein families, G protein-coupled receptors (GPCRs) have yielded about 30 unique structures so far (Shonberg et al. 2014).

GPCRs contain more than 800 members in humans, with about 200 of them being validated drug targets. Due to the low expression and stability of these receptors as well as their highly dynamic nature, they have resisted structural determination for many years and the first high-resolution structure of a GPCR bound to a diffusible ligand was solved by X-ray crystallography only recently in 2007 (Cherezov et al. 2007). This structure, as well as most GPCR structures solved since then, were derived from small but well-ordered crystals grown in a lipidic cubic phase (LCP) (Landau and Rosenbusch 1996; Caffrey and Cherezov 2009). However, the high X-ray flux required to collect high-resolution data from small crystals results in radiation damage (Meents et al. 2010), even in cryo-cooled samples. Radiation damage at synchrotron sources, together with the low-expression yield of membrane proteins and difficulties with growing diffraction quality crystals, remain the major bottleneck in this field (Juers and Matthews 2004).

Radiation damage can however be outrun at X-ray free-electron lasers (XFELs). An XFEL provides ultrashort X-ray pulses with a peak brilliance that is over nine orders of magnitude higher than from third-generation synchrotron sources, enabling structure determination from micrometer- or sub-micrometer-size nanocrystals with minimal radiation damage, based on the principle of "diffraction-before-destruction" (Neutze et al. 2000). The method of serial femtosecond crystallography (SFX) is able to minimize the radiation damage by using those intense and ultrashort pulses to collect a series of snapshot diffraction patterns from microcrystals at room temperature, eliminating the steps of crystal harvesting and cryo-cooling (Chapman et al. 2011; Boutet et al. 2012; Redecke et al. 2013). The diffraction snapshots originate from different crystals in random orientation and differing in size. These diffraction patterns constitute "stills", i.e. slices through the Ewald sphere containing only partial Bragg reflections. Therefore tens of thousands snapshots from crystals in random orientation are typically needed to adequately sample reciprocal space.

In this chapter, we will review the recent evolution of serial femtosecond crystallography, the application of SFX on membrane proteins, and an innovative modified LCP-SFX approach combining SFX and LCP crystallisation.

11.2 Challenges in Structure Determination of Membrane Proteins

Membrane proteins are relatively unstable once isolated from their native lipid bilayer membrane environment. Their crystallization in detergent micelles often leads to large but poorly diffracting crystals. In contrast, crystals grown in LCP are typically smaller in size, more ordered and

contain fewer defects that contribute to mosaicity (Cherezov 2011). The high X-ray dose at conventional synchrotron sources leads to radiation damage and associated structure modification. To address this issue, cryogenic cooling of microcrystalline samples is used (Meents et al. 2010), where the crystal is cooled to 100 K to reduce secondary radiation damage whereas primary ionization events cannot be prevented (Meents et al. 2010; Juers and Matthews 2004).

Overall, structural studies of membrane proteins are hampered by the initial crystal quality as well as the limited growth capacity to large well-ordered crystals withstanding radiation damage.

11.3 History of Serial Femtosecond Crystallography

To overcome X-ray-induced radiation damage, it was proposed to use extremely intense X-ray pulses with short enough pulse duration that diffraction data can be recorded before the structural destruction occurs (Solem 1986). The first hard X-ray FEL, the Linac Coherent Light Source (LCLS) at SLAC in Stanford allowed to test these ideas for the first time (Emma et al. 2010). Together with fast-readout detectors and sample delivery in a liquid stream, short-wavelength X-ray pulses with high intensity at LCLS enabled for the first time high-resolution structure determination of protein molecules at room temperature from nano- and microcrystals. Photosystem I (PSI) was used as the first crystallographic experimental model at LCLS (Chapman et al. 2011). In this experiment, randomly orientated hydrated microcrystals in crystallisation solution were delivered in a liquid jet (DePonte et al. 2008), and intersected with the X-ray beam in vacuum. Thousands of single femtosecond snapshot diffraction patterns from microcrystals were collected in a serial fashion. New data analysis methods had to be developed to merge the resulting "still" images into a 3D data set (Kirian et al. 2010). Although the X-ray wavelength was limited at the time to 6.9 Å, which in turn limited the resolution of the PSI structure to 8.4 Å, it was a first step towards atomic resolution SFX with an XFEL. Data collection to a resolution better than 2 Å became possible with the commissioning of the LCLS Coherent X-ray Imaging (CXI) instrument. The model system for this study was hen egg-white lysozyme and the structure could be solved from micron sized crystals to a resolution of 1.9 Å with an X-ray wavelength of 1.32 Å (Boutet et al. 2012). Since then, the LCLS has been used for SFX structure determination of soluble and membrane proteins (Aquila et al. 2012; Johansson et al. 2012; Kern et al. 2012; Liu et al. 2013; Kupitz et al. 2014; Weierstall et al. 2014).

11.4 The Emergence of Serial Femtosecond Crystallography as a Tool for Structural Studies of Membrane Proteins

In serial femtosecond crystallography, extremely short X-ray pulses with high energy intersect a stream of protein microcrystals in random orientation and variable size (Chapman et al. 2011). At the LCLS, depending on crystal concentration, up to 120 "still" diffraction patterns from different crystals are recorded per second. After recording and indexing thousands of patterns, a Monte Carlo integration yields the structure factors in a format suitable for standard crystallography software (Kirian et al. 2011).

Following the first success of SFX on PSI crystallized in detergent solution (Chapman et al. 2011). SFX was applied to the structural studies of other membranes proteins, such as the photosynthetic reaction center from *Blastochloris viridis* (RCvir) that was crystallised in a liquid-like lipidic sponge phase (Johansson et al. 2012). This study was still limited by the wavelength of 6.17 Å that was available at the time, resulting in an 8.2 Å resolution structure of RCvir. A follow up SFX study on the same protein, but at higher X-ray energy of 9.34 keV corresponding to a wavelength of 1.32 Å led to a 3.5 Å resolution structure (Johansson et al. 2013).

In order to minimise microcrystal sample waste and achieve high hit rate, a well-designed sample delivery system is essential, which streams microcrystals in their crystallisation

environment into the intersection with the pulsed XFEL beam.

Currently, two liquid sample delivery systems have been developed and used for SFX data collection. The most used so far is the gas dynamic virtual nozzle (GDVN) injector, which generates a continuous liquid stream of 1–20 μm diameter (DePonte et al. 2008). In the GDVN, the liquid containing protein microcrystals is focused by a sheath gas to a small diameter ("virtual aperture"), thereby avoiding clogging problems associated with "real" apertures (DePonte et al. 2008). The flow rate necessary to sustain continuous jetting with a GDVN nozzle is about 7 $\mu l \cdot min^{-1}$, which results in high sample consumption and sample waste, since at the current LCLS repetition rate of 120 Hz most sample runs to waste in between X-ray pulses, requiring 10–100 mg of crystallised protein for a complete dataset collection. Nevertheless, this type of injector has been successfully used for several structural studies of membrane proteins (Chapman et al. 2011; Johansson et al. 2012, 2013; Kupitz et al. 2014).

A second injector uses the principle of electrospinning, where the liquid is subjected to a 3.4–5.4 $kV \cdot cm^{-1}$ electric field. The high field generates a liquid meniscus (Taylor cone) similar as in Electrospray, but in electrospinning droplet formation is delayed by adding glycerol and/or polyethylene glycol and an unbroken stream of charged liquid is produced. This system has been used to deliver microcrystals inside a vacuum chamber with a flow rate of 0.17–3.1 $\mu l\ min^{-1}$ (Kern et al. 2012; Sierra et al. 2012). A caveat of this method is, that it requires the addition of a cryoprotectant to prevent freezing of the liquid in vacuum.

11.5 Serial Femtosecond Crystallography of Membrane Proteins in Lipidic Cubic Phase

Lipidic cubic phase represents a membrane-mimetic material that supports crystal growth of membrane proteins. While crystals that grow in LCP are typically small, they are usually well-ordered. Optimisation of crystallisation condition in LCP to obtain sufficiently large crystals suitable for conventional synchrotron X-ray crystallography is a time-consuming process. Small crystals in LCP are therefore ideal for serial femtosecond crystallography at XFELs, which eliminates many crystal optimisation steps and crystal harvesting.

The high viscosity and gel-like consistency of LCP allows efficient microcrystal delivery without much sample waste in a stream of LCP produced by a special injector, which is described next in the chapter (Weierstall et al. 2014). Acquisition of a complete dataset by the LCP-SFX method requires several tens of microlitres of LCP with homogenously dispersed microcrystals at high density. An optimized protocol of microcrystal preparation for LCP-SFX was recently published (Liu et al. 2014). Initial crystal hits are acquired from the nanoliter volume high-throughput robotic screening of LCP crystallization conditions in 96-well glass sandwich plates (Cherezov et al. 2004). Successful conditions producing high-density of small crystals are then scaled up by approximately 1000-times inside gas-tight Hamilton syringes (Fig. 11.1).

The most common host lipid for LCP crystallisation is monoolein, or 9.9 MAG (a monoacylglycerol with 9 hydrocarbons before and 9 after a single double bond). It was observed that using monoolein-based LCP might lead to a problem when sample is injected into a vacuum chamber. Evaporative cooling and dehydration transforms LCP into a lamellar crystalline phase, which produces strong diffraction rings that can damage the detector. To overcome this, 7.9 MAG lipid that was designed for low temperature crystallisation (Misquitta et al. 2004) can be added to the sample after crystals have grown (Liu et al. 2014).

11.6 Microcrystal Sample Delivery System in LCP-SFX

In order to generate a micron sized stream of LCP which has a dynamic viscosity of ~48.3 Pas (Perry et al. 2009), it was necessary to develop a new device, since the GDVN nozzle cannot be used with such high viscosity materials. The

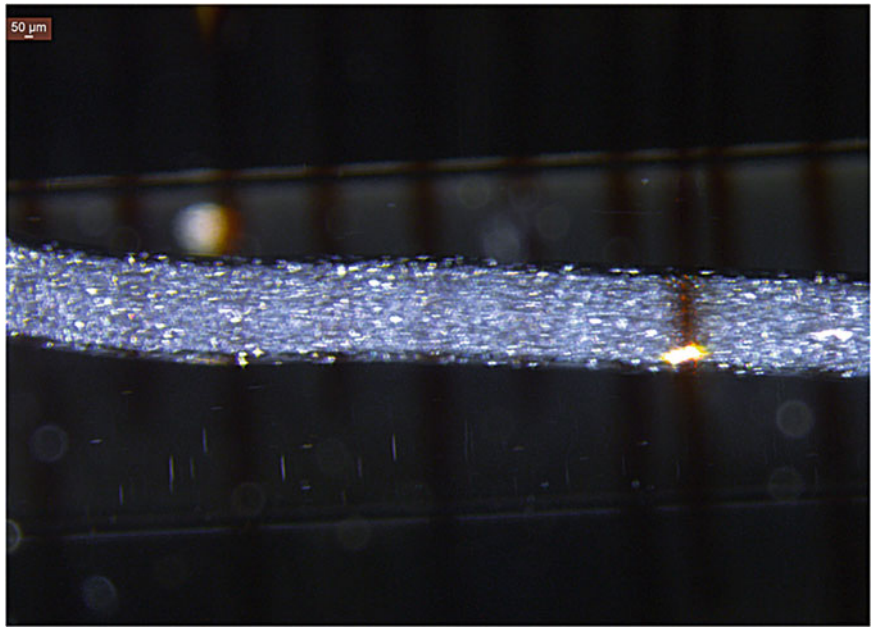

Fig. 11.1 Cross-polarized image of Angiotensin II receptor type 1 (AT1R) LCP microcrystals grown in gas-tight Hamilton syringes

goal was to design a system that can reliably extrude a viscous stream of 10–50 µm diameter at variable speed adjustable to the X-ray pulse repetition rate. The injection process has to be reliable at both vacuum and ambient pressures (e.g. in Helium atmosphere), since XFEL experiments are often conducted in vacuum to reduce background scattering. The stream speed has to be adjustable in the range of about 10 µm/s to 3 mm/s to allow the damaged sample to be replenished by fresh sample for X-ray pulse repetition rates of 10–120 Hz.

The final design of the LCP injector is shown in Fig. 11.2 and consists of a hydraulic stage, a sample reservoir and a nozzle. The hydraulic stage comprises a syringe body containing a sealed solid piston. The injector piston, which is driven forward with water pushed by an HPLC pump, compresses a pair of Teflon balls, which driven by a pressure-amplification stage, extrude the LCP sample through a 10–50 µm inner diameter (ID) capillary. The hydraulic piston has a large diameter on the inlet side and a much smaller diameter on the outlet side. The ratio of the respective bore areas gives a nominal pressure amplification factor of 34, delivering 10,200 psi to the LCP reservoir when hydraulic fluid (water) on the inlet side is pressurized to 300 psi. Two different size sample reservoirs are available, which can hold up to 25(45) µl of LCP. The reservoir bore is filled with LCP via a Hamilton syringe. On the piston side, the reservoir is sealed by a Teflon ball. On the nozzle side, the sample reservoir is connected to a fused silica capillary with 10–50 µm inner diameter. The capillary is kept as short as possible (6 cm) to reduce the pressure necessary for LCP extrusion.

The LCP is extruded out of this capillary into an evacuated sample chamber (or a helium filled chamber); sample extrusion requires a pressure of 2,000–10,000 psi depending on the nozzle diameter, flow speed, and sample viscosity. Shear force exerted by a co-flowing gas (helium or nitrogen at 300–500 psi supply pressure) keeps the LCP stream on axis. To generate the co-flowing gas stream, the tapered end of the sample capillary is inserted into a flame-polished square glass tube and protrudes out of the square exit aperture, so that gas can flow through the open corners at a rate adequate for LCP extrusion (Fig. 11.3).

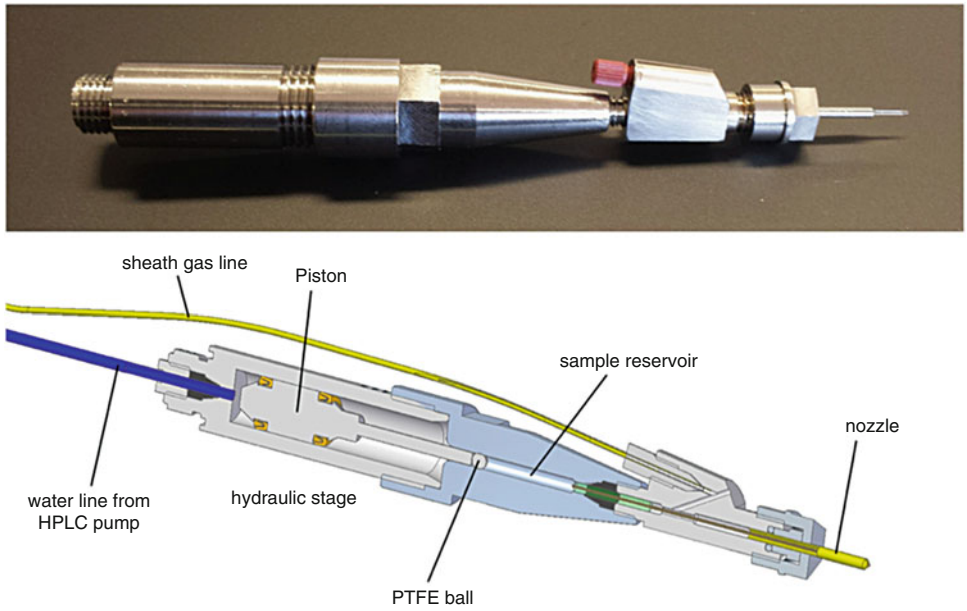

Fig. 11.2 *Top*: LCP injector. The device is about 12 cm long. *Bottom*: Cross-sectional view of the LCP injector

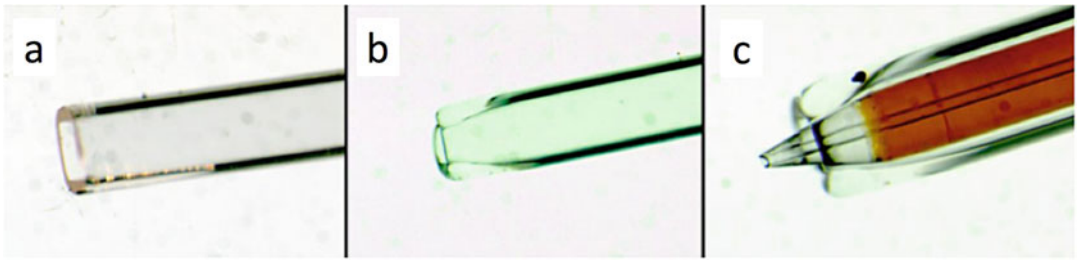

Fig. 11.3 LCPnozzle: (**a**) Square gas aperture before melting (**b**) after melting (**c**) with sample capillary of 50 μm ID protruding out of the melted gas aperture

The LCP flow rate can be optimized for the 10–120 Hz pulse repetition rate of the LCLS so that between X-ray pulses, the stream advances only the distance needed to expose fresh sample to the next pulse. The used repetition rate depends on the detector used, e.g. the CSPAD detector (Hart et al. 2012) currently in use at CXI is highly sensitive and has low dynamic range, but allows the use of the maximum 120 Hz repetition rate. The necessary distance the LCP stream has to advance between pulses (the 'damage diameter') depends on the X-ray beam diameter, LCP stream diameter and pulse energy. Thus, for example, at an X-ray energy of 9.5 keV, a pulse energy of 50 mJ at the sample and a beam diameter of 1.5 μm, this distance is 10–30 μm. Consequently, for a flow speed where the LCP stream travels 10–30 μm between X-ray pulses (1.2–3.6 mm/s), little, if any, sample is wasted and sample consumption is reduced dramatically compared with GDVN injection. Constant LCP flow rates of 1–300 nL/min can be achieved by adjusting the flow rate setting on the HPLC pump.

11.7 LCP-SFX Structures of Membrane Proteins

The LCP-SFX method was initially validated by comparing structures of the human serotonin 5-HT_{2B} receptor bound to an agonist ergotamine (ERG), solved by using traditional microcrys-

tallography at a synchrotron source (5-HT_{2B}-SYN) (Wacker et al. 2013) and by SFX at the Coherent X-ray Imaging (CXI) instrument of LCLS (5-HT_{2B}-XFEL) (Liu et al. 2013). Both structures were determined at a similar resolution, 2.8 Å for the 5-HT_{2B}-XFEL structure and 2.7 Å for the 5-HT_{2B}-SYN, however, major differences were involved in the way how the data were collected and processed. The 5-HT_{2B}-XFEL data were collected at room temperature using microcrystals with an average size of $5 \times 5 \times 5$ μm streamed inside LCP medium, in which they have been grown, and intersecting in random orientations with the 1.5 μm in diameter XFEL pulses of 50 fs duration and 120 Hz repetition rate. Overall, 32,819 microcrystals contributed to the final dataset that was processed by the CrystFEL program (White et al. 2013). By comparison, the 5-HT_{2B}-SYN dataset was collected from cryo-cooled crystals of an average size of $80 \times 20 \times 10$ μm by taking oscillation patterns upon crystal exposure with a 10 μm in diameter synchrotron beam. Due to the crystal sensitivity to radiation damage, 17 crystals were required to obtain a complete dataset, and the data were processed by the HKL2000 program (Otwinowski and Minor 1997). Both structures were solved by molecular replacement (MR) and refined by Phenix (Adams et al. 2010) using the same parameters, and displayed high-quality electron density maps for most residues of 5-HT_{2B}, the agonist ergotamine, covalently attached palmitic acid, cholesterol and several lipid and water molecules.

Despite the very different methods of data acquisition and processing, both structures displayed almost identical backbone trace (Cα atoms RMSD = 0.46 Å excluding flexible N-terminus and parts of extracellular loop 2), validating the LCP-SFX protocols. While overall similar, several deviations between these two structures were noticed. First, the unit cell volume of 5-HT_{2B}-SYN was 2.1 % smaller than the one of 5-HT_{2B}-XFEL, consistent with the shrinkage of crystal lattice induced by cryo-cooling. Several side chains showed different rotamer conformations between these two structures, potentially due to the cryo-cooling-induced partial remodelling (Fraser et al. 2011). The average B-factor of 5-HT_{2B}-XFEL structure was 21 $Å^2$ larger than that of 5-HT_{2B}-SYN structure, consistent with the increased thermal motions at room temperature. Furthermore, the extracellular tip of helix II formed an α-helix instead of a water-stabilized kink in 5-HT_{2B}-SYN structure. Most of these discrepancies observed between the 5-HT_{2B}-XFEL and 5-HT_{2B}-SYN structures were attributed to the differences in data collection temperature (Juers and Matthews 2004). The LCP-SFX therefore enabled determination of the first room temperature GPCR structure, providing more accurate insights into receptor structure and function at close to native conditions.

After successful validation, the LCP-SFX method was applied to solve the structure of the human smoothened receptor (SMO) in complex with cyclopamine (Weierstall et al. 2014). SMO belongs to the Frizzled family GPCRs and participates in the embryonic development and growth of cancer cells. Blockade of the SMO receptor by small molecule antagonists is considered a promising strategy for the treatment of certain tumors. Cyclopamine is a small molecule, SMO antagonist (Chen et al. 2002), produced by corn lily, which was discovered during an epidemic of cyclopia in newborn lambs at an Idaho farm. In efforts to determine the structure of SMO in complex with cyclopamine, relatively large crystals were produced in LCP and tested at a synchrotron beamline. These crystals, however, produced poor diffraction with high mosaicity and anisotropy. On the contrary, much smaller crystals grown in similar conditions did not suffer from high mosaicity and were used to determine the SMO-cyclopamine structure at 3.2 Å resolution by LCP-SFX at LCLS. The electron density clearly revealed the location of cyclopamine in the long and narrow crevice inside SMO.

In early 2015 this method was used to determine the structure of the human δ-opioid receptor bound to a bifunctional peptide DIPP-NH_2 at 2.7 Å resolution (Fenalti et al. 2015). Bifunctional ligands acting as agonists towards μ-opioid receptor and antagonist towards δ-

opioid receptor are promising alternatives to opiate painkillers, frequent administration of which do not lead to acquiring tolerance and dependency. Finally, most recently the LCP-SFX method enabled structure determination of the first novel GPCR, the human angiotensin II receptor type 1 (AT1R), a blood pressure regulator, in complex with an angiotensin receptor blocker (Zhang et al. 2015).

11.8 Summary and Outlook for Serial Femtosecond Crystallography in LCP

Within relatively short time since the emergence of the first hard XFEL source, it is becoming increasingly clear that serial femtosecond crystallography has the potential to accelerate structural studies of membrane proteins under more native conditions, which is highly critical for identifying structure-function relationships of membrane proteins. The innovative approach described in this chapter of using LCP crystallisation to obtain well-ordered high-quality microcrystals suitable for data collection by serial femtosecond crystallography with highly intense and ultrashort XFEL pulses has already yielded several room-temperature high-resolution structures of challenging membrane proteins (Liu et al. 2013; Weierstall et al. 2014; Fenalti et al. 2015; Zhang et al. 2015).

Compared with traditional X-ray crystallography, SFX practically eliminates radiation damage that usually occurs when working with small crystals. SFX approach accurately captures structural details at room temperature under physiological conditions, and LCP provides environmental conditions close to the native environment of membrane proteins. Thus, the combination of XFEL (Emma et al. 2010; Boutet and Williams 2010), LCP crystallisation (Liu et al. 2014), LCP injector (Weierstall et al. 2014) and fast-readout CSPAD detector (Hart et al. 2012) brings forth a unique approach enabling structural studies of difficult to crystallise membrane proteins.

Continued developments of LCP-SFX will further decrease sample consumption and required crystal size by possibly narrowing the diameter of the LCP stream to reduce the background scattering. This will require continued injector development and better control over the crystallisation process in LCP to obtain a more homogeneous crystal size distribution and thereby avoiding clogs from large crystals. New data processing software developments are already underway which should result in faster data collection using less diffraction patterns (Uervirojnangkoorn et al. 2015; Ginn et al. 2015). Improvements in detectors will allow to use higher X-ray fluence, since current detectors have limited dynamic range and require significant attenuation of the X-ray intensity to prevent saturation by strong Bragg peaks. Finally, it should be possible to look at conformational changes in protein crystals delivered in LCP (molecular movies) similar to the recent seminal studies with liquid injectors (Tenboer et al. 2014).

Acknowledgments This work was supported in parts by the NIH grants R01 GM108635 and U54 GM094618 (V.C.), NSF BioXFEL Science and Technology center grant 1231306 (U.W. and W.L.). Further supports were provided by the Arizona State University (ASU) Biodesign Seed Grant Program and ASU-Mayo Seed Grant Program (L.Z. and W.L.). Parts of this research were carried out at the LCLS, a National User Facility operated by Stanford University on behalf of the U.S. Department of Energy, Office of Basic Energy Sciences, and at the GM/CA CAT of the Argonne Photon Source, Argonne National Laboratory.

References

Adams PD, Afonine PV, Bunkoczi G, Chen VB, Davis IW, Echols N et al (2010) PHENIX: a comprehensive Python-based system for macromolecular structure solution. Acta Crystallogr D Biol Crystallogr 66(2):213–221

Aquila A, Hunter MS, Doak RB, Kirian RA, Fromme P et al (2012) Time-resolved protein nanocrystallography using an X-ray free-electron laser. Opt Express 20(3):2706–2716

Boutet S, Williams GJ (2010) The coherent X-ray imaging (CXI) instrument at the Linac coherent light source (LCLS). New J Phys 12:035024

Boutet S, Lomb L, Williams GJ, Barends TR, Aquila A et al (2012) High-resolution protein structure determination by serial femtosecond crystallography. Science 337:362–364

Caffrey M, Cherezov V (2009) Crystallizing membrane proteins using lipidic mesophases. Nat Protocols 4:706–731

Chapman HN, Fromme P, Barty A, White TA, Kirian RA, Aquila A et al (2011) Femtosecond X-ray protein nanocrystallography. Nature 470:773–777

Chen JK, Taipale J, Cooper MK, Beachy PA (2002) Inhibition of Hedgehog signaling by direct binding of cyclopamine to Smoothened. Genes Dev 16:2743–2748

Cherezov V (2011) Lipidic cubic phase technologies for membrane protein structural studies. Curr Opin Struct Biol 21(4):559–566

Cherezov V, Peddi A, Muthusubramaniam L, Zheng YF, Caffrey M (2004) A robotic system for crystallizing membrane and soluble proteins in lipidic mesophases. Acta Crystallogr D Biol Crystallogr 60(10):1795–1807

Cherezov V, Rosenbaum DM, Hanson MA, Rasmussen SG, Thian FS, Kobilka TS et al (2007) High-resolution crystal structure of an engineered human beta2-adrenergic G protein-coupled receptor. Science 318:1258–1265

Deisenhofer J, Epp O, Miki K, Huber R, Michel H (1985) Structure of the protein subunits in the photosynthetic reaction centre of Rhodopseudomonas viridis at 3A resolution. Nature 318:618–624

DePonte DP, Weierstall U, Schmidt K, Warner J, Starodub D, Spence JCH, Doak RB (2008) Gas dynamic virtual nozzle for generation of microscopic droplet streams. J Phys D Appl Phys 41:195505

Emma P, Akre R, Arthur J, Bionta R, Bostedt C, Bozek J et al (2010) First lasing and operation of an ångstrom-wavelength free-electron laser. Nat Photonics 4:641–647

Fenalti G, Zatsepin NA, Betti C, Giguere P, Han GW, Ishchenko A et al (2015) Structural basis for bifunctional peptide recognition at human delta-opioid receptor. Nat Struct Mol Biol 22:265–268

Fraser JS, van den Bedem H, Samelson AJ, Lang PT, Holton JM, Echols N, Alber T (2011) Accessing protein conformational ensembles using room-temperature X-ray crystallography. Proc Natl Acad Sci U S A 108:16247–16252

Ginn HM, Messerschmidt M, Ji X, Zhang H, Axford D, Gildea RJ et al (2015) Structure of CPV17 polyhedrin determined by the improved analysis of serial femtosecond crystallographic data. Nat Commun 6:6435

Hart P, Boutet S, CarmI G, Dragone A, Duda B, Freytag D et al (2012) The Cornell-SLAC pixel array detector at LCLS. Ieee nuclear science symposium and medical imaging conference record. Symposium and Medical Imaging Conference (NSS/MIC), IEEE, pp 538–541

Johansson LC, Arnlund D, White TA, Katona G, DePonte DP, Weierstall U et al (2012) Lipidic phase membrane protein serial femtosecond crystallography. Nat Methods 9:263–265

Johansson LC, Arnlund D, Katona G, White TA, Barty A, DePonte DP et al (2013) Structure of a photosynthetic reaction centre determined by serial femtosecond crystallography. Nat Commun 4:2911

Juers DH, Matthews BW (2004) Cryo-cooling in macromolecular crystallography: advantages, disadvantages and optimization. Q Rev Biophys 37:105–119

Kern J, Alonso-Mori R, Hellmich J, Tran R, Hattne J, Laksmono H et al (2012) Room temperature femtosecond X-ray diffraction of photosystem II microcrystals. Proc Natl Acad Sci U S A 109:9721–9726

Kirian RA, Wang X, Weierstall U, Schmidt KE, Spence JC, Hunter M et al (2010) Femtosecond protein nanocrystallography-data analysis methods. Opt Express 18:5713–5723

Kirian RA, White TA, Holton JM, Chapman HN, Fromme P, Barty A et al (2011) Structure-factor analysis of femtosecond microdiffraction patterns from protein nanocrystals. Acta Crystallogr Sect A 67(2):131–140

Kupitz C, Basu S, Grotjohann I, Fromme R, Zatsepin NA, Rendek KN et al (2014) Serial time-resolved crystallography of photosystem II using a femtosecond X-ray laser. Nature 513:261–265

Landau EM, Rosenbusch JP (1996) Lipidic cubic phases: a novel concept for the crystallization of membrane proteins. Proc Natl Acad Sci U S A 93:14532–14535

Liu W, Chun E, Thompson AA, Chubukov P, Xu F, Katritch V et al (2012) Structural basis for allosteric regulation of GPCRs by sodium ions. Science 337:232–236

Liu W, Wacker D, Gati C, Han GW, James D, Wang D et al (2013) Serial femtosecond crystallography of G protein-coupled receptors. Science 342:1521–1524

Liu W, Ishchenko A, Cherezov V (2014) Preparation of microcrystals in lipidic cubic phase for serial femtosecond crystallography. Nat Protoc 9:2123–2134

Meents A, Gutmann S, Wagner A, Schulze-Briese C (2010) Origin and temperature dependence of radiation damage in biological samples at cryogenic temperatures. Proc Natl Acad Sci U S A 107:1094–1099

Misquitta Y, Cherezov V, Havas F, Patterson S, Mohan JM, Wells AJ et al (2004) Rational design of lipid for membrane protein crystallization. J Struct Biol 148:169–175

Neutze R, Wouts R, van der Spoel D, Weckert E, Hajdu J et al (2000) Potential for biomolecular imaging with femtosecond X-ray pulses. Nature 406:752–757

Otwinowski Z, Minor W (1997) Processing of X-ray diffraction data collected in oscillation mode. Methods Enzymol (Academic Press) 276:307–326

Perry SL, Roberts GW, Tice JD, Gennis RB, Kenis PJ (2009) Microfluidic generation of lipidic mesophases for membrane protein crystallization. Cryst Growth Des 9:2566–2569

Redecke L, Nass K, DePonte DP, White TA, Rehders D, Barty A et al (2013) Natively inhibited Trypanosoma brucei cathepsin B structure determined by using an X-ray laser. Science 339:227–230

Shonberg J, Kling RC, Gmeiner P, Löber S (2014) GPCR crystal structures: medicinal chemistry in the pocket. Bioorg Med Chem 23:3880–3906

Sierra RG, Laksmono H, Kern J, Tran R, Hattne J, Alonso-Mori R et al (2012) Nanoflow electrospinning serial femtosecond crystallography. Acta Crystallogr D Biol Crystallogr 68:1584–1587

Solem JC (1986) Imaging biological specimens with high-intensity soft x rays. J Opt Soc Am B 3:1551–1565

Tenboer J, Basu S, Zatsepin N, Pande K, Milathianaki D, Frank M et al (2014) Time-resolved serial crystallography captures high-resolution intermediates of photoactive yellow protein. Science 346: 1242–1246

Uervirojnangkoorn M, Zeldin OB, Lyubimov AY, Hattne J, Brewster A et al (2015) Enabling X-ray free electron laser crystallography for challenging biological systems from a limited number of crystals. Elife 4:05421

Wacker D, Wang C, Katritch V, Han GW, Huang XP, Vardy E et al (2013) Structural features for functional selectivity at serotonin receptors. Science 340: 615–619

Wallin E, von Heijne G (1998) Genome-wide analysis of integral membrane proteins from eubacterial, archaean, and eukaryotic organisms. Protein Sci 7:1029–1038

Weierstall U, James D, Wang C, White TA, Wang D, Liu W et al (2014) Lipidic cubic phase injector facilitates membrane protein serial femtosecond crystallography. Nat Commun 5:3309

White TA, Barty A, Stellato F, Holton JM, Kirian RA, Zatsepin NA, Chapman HN (2013) Crystallographic data processing for free-electron laser sources. Acta Crystallogr D Biol Crystallogr 69(7): 1231–1240

Yildirim MA, Goh KI, Cusick ME, Barabási AL, Vidal M (2007) Drug-target network. Nat Biotechnol 25:1119–1126

Zhang H, Unal H, Gati C, Han GW, Liu W, Zatsepin NA et al (2015) Structure of the Angiotensin receptor revealed by serial femtosecond crystallography. Cell 161:833–844